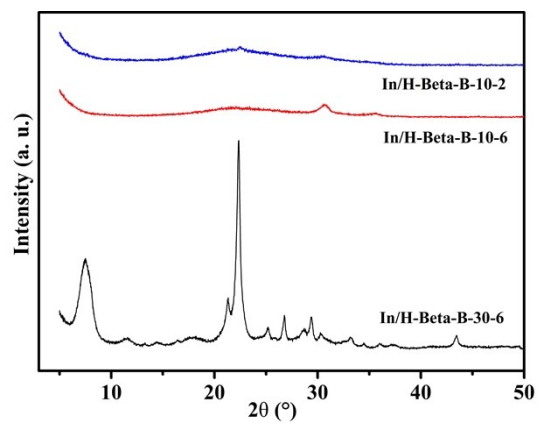
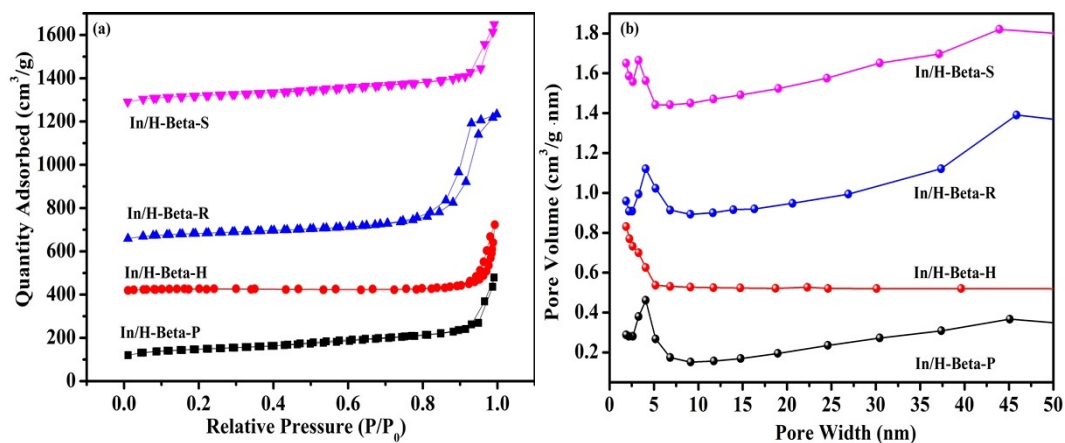


**Fig. S1.** Chemical structural formula of the eight amino acids used in the study.



**Fig. S2.** The XRD patterns of In/H-Beta-B-10-2, In/H-Beta-B-10-6, and In/H-Beta-B-30-6.



**Fig. S3.** (a)  $N_2$  adsorption–desorption isotherms of In/H-Beta-P, In/H-Beta-H, In/H-Beta-R, and In/H-Beta-S samples, the isotherms for In/H-Beta-H, In/H-Beta-R, and In/H-Beta-S are vertically offset by 405, 628, 1169  $cm^3/g$ , respectively and (b) BJH desorption pore distributions of In/H-Beta-P, In/H-Beta-H, In/H-Beta-R, and In/H-Beta-S samples, the those for In/H-Beta-H, In/H-Beta-R, and In/H-Beta-S are vertically offset are 0.5, 0.8, 1.4  $cm^3/g \cdot nm$ , respectively.

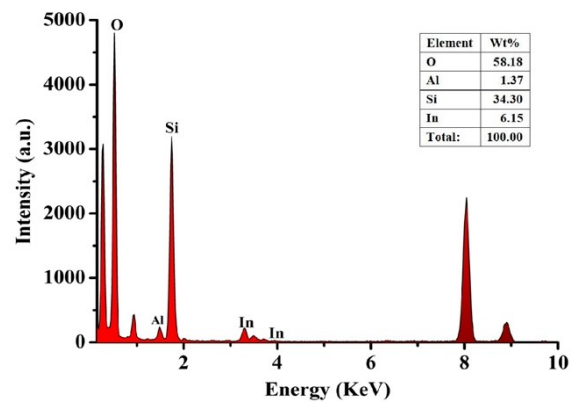


**Fig. S4.** EDX spectrum of In/H-Beta-P catalyst.

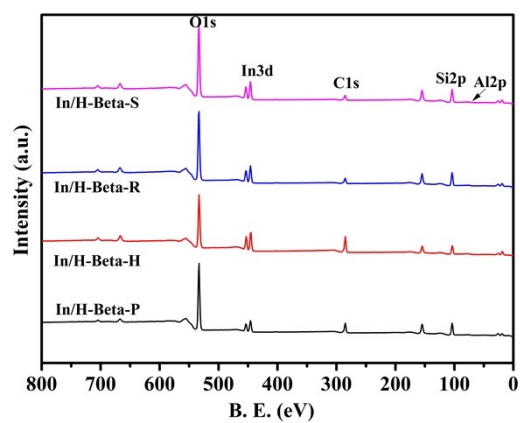


**Fig. S5.** XPS survey spectra of In/H-Beta-P, -H, -R, and -S catalyst.

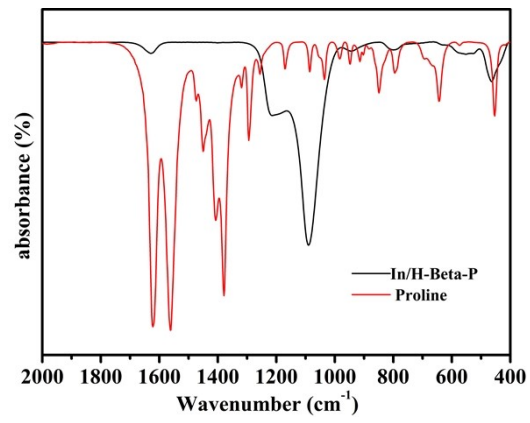


**Fig. S6.** FT-IR spectra of In/H-Beta-P in comparison with pure proline.

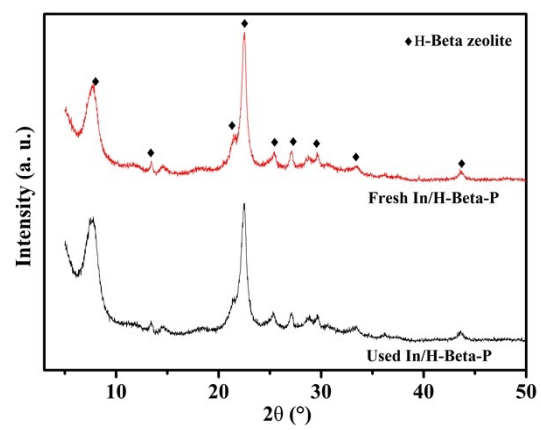


**Fig. S7.** The XRD patterns of fresh and used In/H-Beta-P.